2017 American Control Conference
Sheraton Seattle Hotel
May 24–26, 2017, Seattle, USA

Structural Emergency Control for Power Grids†

Thanh Long Vu, *Member, IEEE,* Spyros Chatzivasileiadis, *Member, IEEE,*
Hsiao-Dong Chiang, *FIEEE,* and Konstantin Turitsyn, *Member, IEEE*

***Abstract*— In this paper, we introduce a structural emergency control to render post-fault dynamics of power systems from the critical fault-cleared state to a stable equilibrium point (EP). Theoretically, this is a new control paradigm that does not rely on any continuous measurement or load shedding, as in the classical setup. Instead, the grid is made stable by intentionally changing the power network structure, and thereby, discretely relocating the EP and its stability region such that the system is consecutively driven from fault-cleared state through a set of EPs to the desired EP. The proposed control is designed by solving convex optimization problems, making it possibly scalable to large-scale power grids. In the practical side, the proposed control can be implemented by exploiting the FACTS devices that will be widely available on the grids, and hence, requiring minor investment.**

Index Terms—Power grids, emergency control, interconnected systems, synchronization

I. Introduction

Large scale level of intermittent renewable generations is installed into power grids, that can compromise the grid's stability, while the low inertia of renewable generators challenges the grid's controllability. As a result, the next-generation power grids will be increasingly vulnerable to unfavorable weather conditions and component failures, which can eventually lead to major outages. Therefore, critical/emergency states of power grids will appear frequently, and thus, emergency control, i.e., the action to recover the stability of a power grid when a critical situation is detected, should be paid serious attention.

Although the existing emergency controls of power grids, such as remedial actions, special protection schemes (SPS), and load shedding [1], [2], make current power grids reasonably stable to disturbances, their drawbacks are twofold. First, some of these emergency actions rely on interrupting electrical service to customers and result in huge economic cost due to power interruptions, e.g. about $79 billion a year in the US [3]. Second, protective devices are usually only effective for individual elements, but less effective in preventing the whole grid from collapse. Recent major blackouts exhibit the inability of operators to prevent grid from cascading failures [4], regardless of the good performance of individual protective devices. The underlying reason is the lack of coordination among protective devices, which makes them incapable of maintaining the stability of the whole grid. These drawbacks call for system-level, cost-effective alternatives to the classical emergency control of power grids.

On the other hand, new generations of smart electronic devices provide fast actuation to smart power grids. Also, transmission resources are continuously installed into the system and will be ubiquitously available in the future. Motivated by the aforementioned observations, this paper aims to extract more value out of the existing and future fast-acting electronic resources and transmission facilities to quickly stabilize the power grid when it is about to lose synchronism after experiencing contingencies (but the voltage is still well-supported). In particular, we propose to use FACTS devices to adjust susceptances of a number of selected transmission lines and/or power injections to thereby stabilize the post-fault power systems.

One of the most remarkably technical difficulties to realize such a control scheme is that the post-fault dynamic of a power grid possesses multiple EPs, each of which has its own stability region (SR), i.e., the set of states from which the post-fault dynamics will converge to the EP. Real-time direct time-domain simulation, which exploits advances in computational hardware, can perform an accurate assessment for post-fault transient dynamics following the contingencies [5]. However, it does not suggest how to properly design the emergency control actions that can surely drive critical/emergency states back to some stable operating condition.

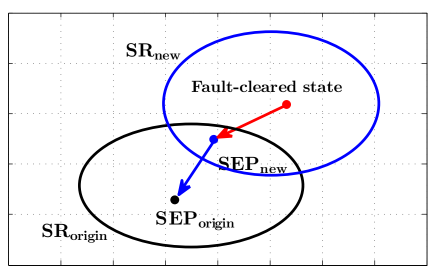

Fig. 1. Stability-driven smart transmission control: the fault-cleared state is made stable by changing the stable equilibrium point (SEP) through adjusting the susceptances of the network transmission lines.

In this paper, will change the transmission network and/or power injection setpoints to obtain a new stable EP such that the fault-cleared state is guaranteed to stay strictly inside the stability region of this new EP, as shown in Fig. 1. Hence, under the new post-fault dynamics, the system trajectory will

† This is a shorten version of our paper titled "Structural emergency control paradigm" which was accepted to publish on the IEEE JETCAS Special Issue on Complex Networks for Modern Smart Grid Applications. This work was supported in part by the MIT/Skoltech initiatives, Ministry of Education and Science of Russian Federation (Grant Agreement 14.615.21.0001) and the National Science Foundation (Contract 1508666). Thanh Long Vu and Konstantin Turitsyn are with MIT, Cambridge, MA, USA, email: {longvu, turitsyn}@mit.edu. Spyros Chatzivasileiadis is with Technical University of Denmark, Copenhagen, Denmark, email: spchatz@elektro.dtu.dk. Hsiao-Dong Chiang is with School of Electrical and Computer Engineering, Cornell University, Ithaca, NY, USA, email: chiang@ece.cornell.edu.

converge from the fault-cleared state to the new EP. If this new EP stays inside the SR of the desired EP, then we recover the original transmission network/power injections and the system state will automatically converge from the new EP to the original EP. Otherwise, this convergence can be performed through a sequence of new transmission control actions which drive the system state to the original EP through a sequence of other EPs as in Fig. 2.

It is worth emphasizing that in the proposed emergency control, we drive the system from the initial state (i.e., the fault-cleared state) to the desired EP by relocating its EP and the corresponding stability region. This setup is unusual from the classical control theory point of view where the EP is usually assumed to be unchanged under the effects of control inputs. Also, we do not require any continuous measurement of any signals, as in the classical control setup.

In this paper, utilizing the Lyapunov function family approach [6], the proposed discrete network changing is designed by solving convex optimization problems, making it possibly scalable to large-scale power grids. In the practical side, the proposed emergency control can be implemented by exploiting the FACTS devices which are widely available on the existing grids, and thus, requires minor investment. In addition, it reduces the need for load shedding causing serious damage to customers in traditional emergency control.

II. Emergency Control Problem

In this paper, we consider power systems under critical situations when the buses' phasor angles may significantly fluctuate but the buses' voltages are still well-supported. For such situations, we utilize the standard structure-preserving model to describe the post-fault dynamics of generators and loads [7]. Mathematically, the gird is described by an undirected graph $\mathcal{A}(\mathcal{N},\mathcal{E})$, where $\mathcal{N} = \{1, 2, \ldots, |\mathcal{N}|\}$ is the set of buses and $\mathcal{E} \subseteq \mathcal{N} \times \mathcal{N}$ is the set of transmission lines connecting those buses. Here, $|A|$ denotes the number of elements in set A. The sets of generator buses and load buses are denoted by $\mathcal{G}$ and $\mathcal{L}$. We assume that the grid is lossless with constant voltage magnitudes $V_k, k \in \mathcal{N}$, and the reactive powers are ignored. Then, the structure-preserving model of the system is given by [7]:

$$m_k\ddot{\delta_k} + d_k\dot{\delta_k} + \sum_{j\in\mathcal{N}_k} a_{kj}\sin(\delta_k-\delta_j) = P_{m_k}, k \in \mathcal{G}, \quad (1a)$$

$$d_k\dot{\delta_k} + \sum_{j\in\mathcal{N}_k} a_{kj}\sin(\delta_k-\delta_j) = -P^0_{d_k}, k \in \mathcal{L}, \quad (1b)$$

where equation (1a) represents the dynamics at generator buses and equation (1b) the dynamics at load buses [8].

The critical situations considered in this paper are when the fault-on trajectory is leaving polytope $\Pi/2$ defined by inequalities $|\delta_{kj}| \le \pi/2, \forall\{k,j\} \in \mathcal{E}$, i.e., the fault-cleared state δ_0 stays outside polytope $\Pi/2$. In normal power systems, protective devices will be activated to disconnect faulted lines/nodes, which will isolate the fault and prevent the post-fault dynamics from instability (this would usually happen at some point beyond a voltage angle difference $\pi/2$).

Avoiding disconnecting line/node, our emergency control objective is to make post-fault dynamics become stable by controlling the post-fault dynamics from the fault-cleared state δ_0 to the stable equilibrium point $\delta^*_{\mathbf{origin}}$, which, e.g., may be an optimum point of some optimal power flow (OPF) problem. To achieve this, we consider adjusting the post-fault dynamics through adjusting the susceptance of some selected transmission lines and/or changing power injections. These changes can be implemented by the FACTS devices available on power transmission grids. The rationale of this control is based on the observation illustrated in Fig. 1 that, by appropriately changing the structure of power systems, we can obtain new post-fault dynamics with a new equilibrium point whose region of attraction contains the fault-cleared state δ_0, and therefore, the new post-fault dynamic is stable.

Formally, we consider the following problem:

(P) **Structural Emergency Control Design:** *Given a fault-cleared state δ_0 and the stable EP $\delta^*_{\mathbf{origin}}$, determine the feasible values for susceptances of selected transmission lines and/or feasible power injection such that the post-fault dynamics are driven from the fault-cleared state δ_0 to the original post-fault EP $\delta^*_{\mathbf{origin}}$.*

III. Fault-Dependent Stability Certificate

In this section, we construct a set of fault-dependent Lyapunov functions that are convex and result in an easy-to-verify stability certificate for assessing the control performance in the next section. First of all, we obtain (see [8]) an equivalent representation of (1) as

$$\dot{x} = Ax - BF(Cx). \quad (2)$$

To certify stability for fault-cleared state staying outside polytope $\Pi/2$, which likely happens in emergency situations, we construct a family of the fault-dependent convex Lyapunov functions. Assume that the fault-cleared state x_0 has a number of phasor differences larger than $\pi/2$. Usually, this happens when the phasor angle at a node becomes significantly large, making the phasor difference associated with it larger than $\pi/2$. Without loss of generality, we assume that $|\delta_{ij}(0)| > \pi/2, \forall j \in \mathcal{N}_i$ at some given node $i \in \mathcal{N}$. Also, it still holds that $|\delta_{ij}(0) + \delta^*_{ij}| \le \pi$ for all $j \in \mathcal{N}_i$. Consider polytope $\mathcal{Q}$ defined by inequalities

$$|\delta_{ij} + \delta^*_{ij}| \le \pi, \forall j \in \mathcal{N}_i,$$
$$|\delta_{kj}| \le \pi/2, \forall j \in \mathcal{N}_k, \forall k \neq i. \quad (3)$$

Hence, the fault-cleared state is inside polytope $\mathcal{Q}$. Inside $\mathcal{Q}$, consider the Lyapunov function family given by

$$V(x) = \frac{1}{2}x^\top Qx - \sum_{\{k,j\}\in\mathcal{E}} K_{\{k,j\}}\left(\cos\delta_{kj} + \delta_{kj}\sin\delta^*_{kj}\right),$$

where the matrices $Q, K \ge 0$ satisfying the following LMIs:

$$\begin{bmatrix} A^\top Q + QA & R \\ R^\top & -2H \end{bmatrix} \le 0, \quad (4)$$

$$Q - \sum_{j\in\mathcal{N}_i} K_{\{i,j\}} C^\top_{\{i,j\}} C_{\{i,j\}} \ge 0, \quad (5)$$

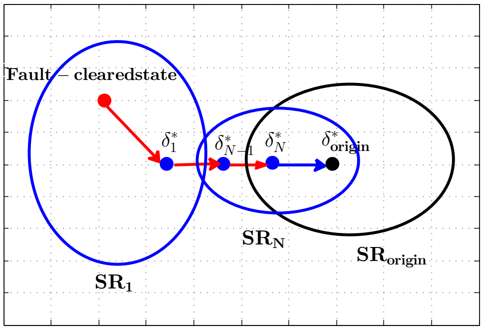

Fig. 2. Selection of stable EPs $\delta_i^*, i = 1, ..., N$, such that the fault-cleared state is driven through the sequence of EPs back to the desired EP $\delta^*_{\mathbf{origin}}$.

where $C_{\{i,j\}}$ is the row of matrix C that corresponds to the row containing $K_{\{i,j\}}$ in the diagonal matrix K. From (3) and (5), we can see that the Hessian of the Lyapunov function inside $\mathcal{Q}$ is positive semidefinite. As such, the Lyapunov function is convex inside $\mathcal{Q}$ and thus, the corresponding minimum value $V_{\min}(\mathcal{Q})$, defined over the flow-out boundary of $\mathcal{Q}$, can be calculated in polynomial time:

$$V_{\min} = V_{\min}(\mathcal{Q}) = \min_{x \in \partial \mathcal{Q}^{out}} V(x). \tag{6}$$

Similar to [6], we can prove that the following set

$$\mathcal{R}_{\mathcal{Q}} = \{x \in \mathcal{Q} : V(x) < V_{\min}\} \tag{7}$$

is an estimate of the stability region.

It is worth noting that LMIs (4)-(5) provide us with a family of Lyapunov functions, characterized by matrices Q and K. For a given fault-cleared state, by an adaptation algorithm similar to that in [6], we can find the best suitable function in this family to certify its stability [9].

IV. Structural Emergency Control Design

In this section, we solve the post-fault emergency control problem **(P)**. As illustrated in Fig. 2, to render the post-fault dynamics from the fault-cleared state x_0 to the EP $\delta^*_{\mathbf{origin}}$, we will find a sequence of stable EPs $\delta_1^*, ..., \delta_N^*$ with their corresponding region of attractions $\mathbf{SR_1}, ..., \mathbf{SR_N}$ such that

$$x_0 \in \mathbf{SR_1}, \delta_1^* \in \mathbf{SR_2}, ..., \delta_{N-1}^* \in \mathbf{SR_N}, \delta_N^* \in \mathbf{SR_{origin}}.$$

Then, the post-fault dynamics can be attracted from the fault-cleared state x_0 to the original EP $\delta^*_{\mathbf{origin}}$ through a sequence of appropriate structural changes in the power network. We will show that we only need to determine a finite number of EPs through solving convex optimization problems.

Recall that, the equilibrium point δ^* is a solution to the power flow-like equations:

$$\sum_{j \in \mathcal{N}_k} V_k V_j B_{kj} \sin \delta^*_{kj} = P_k, \forall k \in \mathcal{N}. \tag{8}$$

As such, the sequence of EPs $\delta_1^*, ..., \delta_N^*$ can be obtained by appropriately changing the susceptances $\{B_{kj}\}$ of the transmission lines or by changing the power injection P_k.

A. Design the first EP by changing power injections

The post-fault dynamics are locally stable when the equilibrium point stays inside the polytope defined by the inequalities $|\delta_{kj}| < \pi/2$. The post-fault dynamics are more stable when the EP is further from the stability margin $|\delta_{kj}| = \pi/2$, i.e., when the phasor differences δ_{kj} are nearer to 0. As such, to search for the EP δ_1^* such that $x_0 \in \mathbf{SR_1}$, we will find the EP δ_1^* such that its phasor differences are as small in magnitude as possible.

We recall in [10] that, for almost all power systems, to make sure $|\delta^*_{kj}| < \gamma < \pi/2$, we need

$$\|L^\dagger p\|_{\mathcal{E},\infty} \le \sin \gamma. \tag{9}$$

Here, $L^\dagger$ is the pseudoinverse of the network Laplacian matrix, $p = [P_1, ..., P_{|\mathcal{N}|}]^\top$, and $\|x\|_{\mathcal{E},\infty} = \max_{\{i,j\}\in\mathcal{E}} |x(i) - x(j)|$. Therefore, to make the phasor differences of the equilibrium point δ_1^* as small as possible, we will find the power injection P_k such that $\|L^\dagger p\|_{\mathcal{E},\infty}$ as small as possible, i.e., minimizing $\|L^\dagger p\|_{\mathcal{E},\infty}$. Note that, with fixed susceptances, the Laplacian matrix $L^\dagger$ is fixed. As such, minimizing $\|L^\dagger p\|_{\mathcal{E},\infty}$ over all possible power injections is a convex optimization problem.

After designing the first EP δ_1^*, we can check if $x_0 \in \mathbf{SR_1}$ by applying the stability certificate presented in the previous section. In particular, given the EP δ_1^* and the fault-cleared state x_0, we can adapt the Lyapunov function family to find a suitable function $V(x)$ such that $V(x_0) < V_{\min}$. A similar adaptation algorithm with what was introduced in [6] can find such a Lyapunov function after a finite number of steps.

B. Design other EPs by changing line susceptances

Now, given the EPs δ_1^* and $\delta^*_{\mathbf{origin}}$, we will design a sequence of stable EPs $\delta_2^*, ..., \delta_N^*$ such that $\delta_1^* \in \mathbf{SR_2}, ..., \delta_{N-1}^* \in \mathbf{SR_N}, \delta_N^* \in \mathbf{SR_{origin}}$. Since all the stable EPs stay inside polytope $\Pi/2$, this design can be feasible.

Case 1: The number of transmission lines that we can change is larger than the number of buses $|\mathcal{N}|$ (i.e., the number of lines with FACTS/PST devices available is larger than $|\mathcal{N}|$), and there are no constraints on the corresponding susceptances. Then, given the EP δ^*, it is possible to solve equation (8) with variables the varying susceptances. Now, we can choose the sequence of stable EPs equi-spaced between the EPs δ_1^* and $\delta^*_{\mathbf{origin}}$, and find the corresponding susceptances. Then we use the presented stability certificate to check if $\delta_1^* \in \mathbf{SR_2}, ..., \delta_{N-1}^* \in \mathbf{SR_N}, \delta_N^* \in \mathbf{SR_{origin}}$.

Case 2: The number of transmission lines that we can change is smaller than the number of buses $|\mathcal{N}|$, or there are some constraints on the corresponding susceptances. Then, it is not always possible to find the suitable susceptances satisfying equation (8) from the given EP δ^*.

In each step, to allow the convergence from δ^*_{i-1} to δ^*_i, we will search over all the reachable susceptance values of selected transmission lines the best one that minimizes the distance from δ^*_{i-1} to δ^*_i. At the same time, we will make the distance from these EPs to the original EP $\delta^*_{\mathbf{origin}}$ strictly decreasing to make sure that only a finite number of EPs is

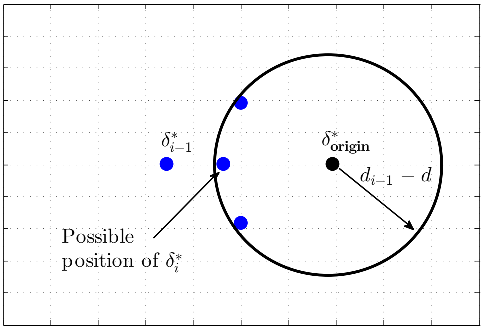

Fig. 3. Localization of δ^*_i as the closest point to δ^*_{i-1} that stays inside the ball around $\delta^*_{\textbf{origin}}$ with the radius $d_{i-1}(\delta^*_{i-1}, \delta^*_{\textbf{origin}}) - d$. The minimization of the distance is taken over all the possible susceptance values of the selected transmission lines. Here, $d > 0$ is sufficiently small such that convergence from δ^*_{i-1} to δ^*_i is guaranteed.

needed. Intuitively, the localization of the EP δ^*_i is shown in Fig. 3. Accordingly, for the reachable set of transmission susceptances, we define δ^*_i as the closest possible EP to δ^*_{i-1} and the distance between δ^*_i and $\delta^*_{\textbf{origin}}$ satisfies

$$d_i(\delta^*_i, \delta^*_{\textbf{origin}}) \leq d_{i-1}(\delta^*_{i-1}, \delta^*_{\textbf{origin}}) - d. \qquad (10)$$

Here, $d > 0$ is a sufficiently small constant chosen such that the convergence from δ^*_{i-1} to δ^*_i is satisfied for all $i = 2, ..., N$, and $d_i(\delta^*_i, \delta)$ is the distance from δ to the equilibrium point δ^*_i, which is defined via $\{B^{(i)}_{kj}\}$, i.e.,

$$\begin{aligned} d_i(\delta^*_i, \delta) &= \sum_{k\in\mathcal{N}} \Big(\sum_{j\in\mathcal{N}_k} V_k V_j B^{(i)}_{kj} (\sin \delta^*_{i_{kj}} - \sin \delta_{kj}) \Big)^2 \\ &= \sum_{k\in\mathcal{N}} \Big(P_k - \sum_{j\in\mathcal{N}_k} V_k V_j B^{(i)}_{kj} \sin \delta_{kj} \Big)^2. \end{aligned}$$

Note that, with $d = 0$, the trivial solution to all of the above optimization problems is $\delta^*_N \equiv ... \equiv \delta^*_2 \equiv \delta^*_1$, and the convergence from δ^*_{i-1} to δ^*_i is automatically satisfied. Nonetheless, since each of the EPs has a nontrivial stability region, there exists a sufficiently small $d > 0$ such that the convergence from δ^*_{i-1} to δ^*_i must still be satisfied for all i.

On the other hand, since $d_i(\delta^*_i, \delta^*)$ is a quadratic function of $\{B^{(i)}_{kj}\}$, defining $\delta^*_2, ..., \delta^*_N$ can be described by the quadratically constrained quadratic program (QCQP):

$$\begin{aligned} &\min_{\{B^{(i)}_{kj}\}} \; d_i(\delta^*_i, \delta^*_{i-1}) \qquad (11) \\ &\textbf{s.t.} \;\; d_i(\delta^*_i, \delta^*_{\textbf{origin}}) \leq d_{i-1}(\delta^*_{i-1}, \delta^*_{\textbf{origin}}) - d. \end{aligned}$$

In optimization problem (11), $d_{i-1}(\delta^*_{i-1}, \delta^*_{\textbf{origin}})$ is a constant obtained from the previous step. Note that, the condition $d_i(\delta^*_i, \delta^*_{\textbf{origin}}) \leq d_{i-1}(\delta^*_{i-1}, \delta^*_{\textbf{origin}}) - d$ will probably place δ^*_i between δ^*_{i-1} and $\delta^*_{\textbf{origin}}$, which will automatically guarantee that δ^*_i stays inside polytope $\Pi/2$. Also, since the equilibrium points are strictly staying inside polytope $\Pi/2$, the functions $d_i(\delta^*_i, \delta^*_{i-1})$ and $d_i(\delta^*_i, \delta^*_{\textbf{origin}})$ are strictly convex functions of $\{B^{(i)}_{kj}\}$. As such, QCQP (11) is convex and can be quickly solved using convex optimization solvers.

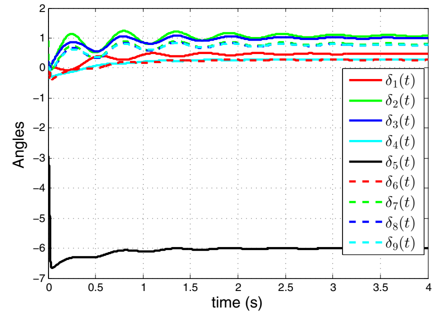

Fig. 4. Buses angular dynamics when the proposed control is not employed

When all of these optimization problems are feasible, then with $d > 0$ from Eqs. (10), we have

$$\begin{aligned} d_1(\delta^*_1, \delta^*_{\textbf{origin}}) &\geq d_2(\delta^*_2, \delta^*_{\textbf{origin}}) + d \geq ... \\ &\geq d_N(\delta^*_N, \delta^*_{\textbf{origin}}) + (N-1)d. \qquad (12) \end{aligned}$$

Hence, $N \leq 1 + (d_1(\delta^*_1, \delta^*_{\textbf{origin}})/d)$, i.e., there is only a finite number of EQs $\delta^*_2, ..., \delta^*_N$ to be determined.

V. Numerical validation

Consider the 9-bus 3-machine system with 3 generator buses and 6 load buses as in [8]. The susceptances of the transmission lines are as follows [11]: $B_{14} = 17.3611 p.u., B_{27} = 16.0000 p.u., B_{39} = 17.0648 p.u., B_{45} = 11.7647 p.u., B_{57} = 6.2112 p.u., B_{64} = 10.8696 p.u., B_{78} = 13.8889 p.u., B_{89} = 9.9206 p.u., B_{96} = 5.8824 p.u.$ The parameters for generators: $m_1 = 0.1254$, $m_2 = 0.034$, $m_3 = 0.016$, $d_1 = 0.0627$, $d_2 = 0.017$, $d_3 = 0.008$. For simplicity, let $d_k = 0.05, k = 4 \ldots, 9$.

Assume that the fault trips the line between buses 5 and 7 and make the power injection variate. When the fault is cleared this line is re-closed. We also assume the fluctuation of the generation (probably due to renewables) and load such that the bus voltages V_k, mechanical inputs P_{m_k}, and steady state load $-P^0_{d_k}$ of the post-fault dynamics after clearing the fault are given in Tab. I. The stable operating condition is calculated as $\delta^*_{\textbf{origin}} = [-0.1629\ 0.4416\ 0.3623\ -0.3563\ -0.3608\ \ -0.3651\ 0.1680\ 0.1362\ 0.1371]^\top, \dot{\delta}^*_{\textbf{origin}} = 0$. However, the fault-cleared state, with angles $\delta_0 = [0.025\ -0.023\ 0.041\ 0.012\ \ -2.917\ \ -0.004\ 0.907\ 0.021\ 0.023]^\top$ and generators angular velocity $[-0.016\ \ -0.021\ 0.014]^\top$, stays outside polytope $\Pi/2$. By our adaptation algorithm, we do not find a suitable Lyapunov function certifying the convergence of this fault-cleared state to the original equilibrium point $\delta^*_{\textbf{origin}}$, so this fault-cleared state may be unstable. We will design emergency control actions to bring the post-fault dynamics from the possibly unstable fault-cleared state to the equilibrium point $\delta^*_{\textbf{origin}}$. All the convex optimization problems will be solved by CVX software.

1) Designing the first EP: Assume that the three generators 1-3 are dispatchable and terminal loads at buses 4-6 are controllable, while terminal loads at the other buses are fixed. We design the first EP by changing the power injections of the three generators 1-3 and load buses 4-6. With the original power injection, $\|L^\dagger p\|_{\mathcal{E},\infty} = 0.5288$.

Node	V (p.u.)	P_k (p.u.)
1	1.0284	3.6466
2	1.0085	4.5735
3	0.9522	3.8173
4	1.0627	-3.4771
5	1.0707	-3.5798
6	1.0749	-3.3112
7	1.0490	-0.5639
8	1.0579	-0.5000
9	1.0521	-0.6054

TABLE I

BUS VOLTAGES, MECHANICAL INPUTS, AND STATIC LOADS.

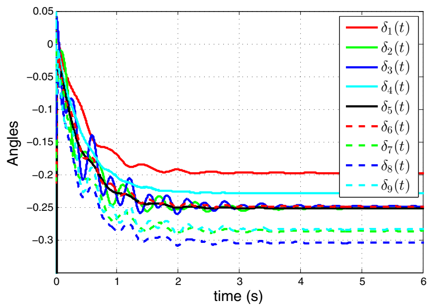

Fig. 5. Effect of power injection control: Convergence of buses angles from the fault-cleared state to δ_1^* in the post-fault dynamics

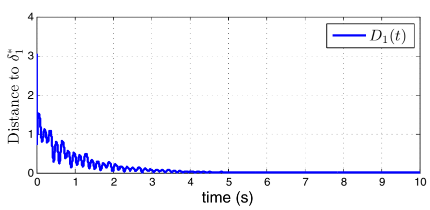

Fig. 6. Effect of injection control: the convergence of the distance $D_1(t)$ to 0. Here, the Euclid distance $D_1(t)$ between a post-fault state and the first equilibrium point δ_1^* is defined as $D_1(t) = \sqrt{\sum_{i=2}^{9}(\delta_{i1}(t) - \delta^*_{1_{i1}})^2}$.

Minimizing $\|L^\dagger p\|_{\mathcal{E},\infty}$ we obtain the new power injections at buses 1-6 as follows: $P_1 = 0.5890, P_2 = 0.5930, P_3 = 0.5989, P_4 = -0.0333, P_5 = -0.0617,$ and $P_6 = -0.0165$. Accordingly, the minimum value of $\|L^\dagger p\|_{\mathcal{E},\infty} = 0.0350 < \sin(\pi/89)$. Hence, the first EP obtained from equation (8) will stay in the polytope defined by the inequalities $|\delta_{kj}| \leq \pi/89, \forall\{k,j\} \in \mathcal{E}$, and can be approximated by $\delta_1^* \approx L^\dagger p = [0.0581\ 0.0042\ 0.0070\ 0.0271\ 0.0042\ 0.0070\ -0.0308\ -0.0486\ -0.0281]^\top$.

Using the adaptation algorithm presented in [6], after some steps we find that there is a Lyapunov function in this family such that $V(x_0) < V_{\min}$. As such, when we turn on the new power injections, the post-fault trajectory will converge from the fault-cleared state x_0 to the new EP δ_1^*. Then, we switch power injections to the original values.

2) Designing the other EPs by changing transmission susceptances: Using the adaptation algorithm, we do not find a suitable Lyapunov function certifying that $\delta_1^* \in \mathbf{SR_{origin}}$. As such, the new EP δ_1^* may stay outside the stability region of the original EP $\delta^*_{\mathbf{origin}}$. We design the impedance adjustment controllers to render the post-fault dynamics from the new EP back to the original EP.

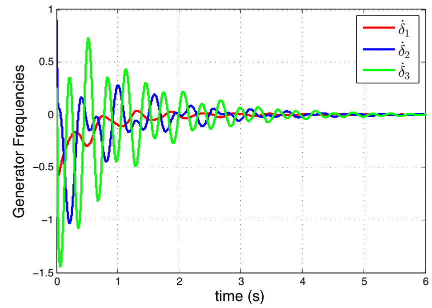

Fig. 7. Generators frequencies under power injection control

Assume that the impedances of transmission lines $\{1,4\},\{2,7\},\{3,9\}$ can be adjusted by FACTS devices. The distance from the first equilibrium point to the original equilibrium point is calculated as $d_1(\delta_1^*, \delta^*_{\mathbf{origin}}) = 70.6424$. Let $d = d_1(\delta_1^*, \delta^*_{\mathbf{origin}})/2 + 1 = 36.3212$, and solve the following convex QCQP with variable $B_{14}^{(2)}, B_{27}^{(2)}$, and $B_{39}^{(2)}$:

$$\min_{\{B_{kj}^{(2)}\}} \; d_2(\delta_2^*, \delta_1^*) \tag{13}$$
$$\text{s.t. } d_2(\delta_2^*, \delta^*_{\mathbf{origin}}) \leq d_1(\delta_1^*, \delta^*_{\mathbf{origin}}) - d = 34.3212.$$

Solving this convex QCQP problem, we obtain the new susceptances at transmission lines $\{1,4\},\{2,7\},\{3,9\}$ as $B_{14}^{(2)} = 33.4174p.u., B_{27}^{(2)} = 22.1662p.u.,$ and $B_{39}^{(2)} = 24.3839p.u.$, with which the distance from the second EP to the first EP and the original EP are given by $d_2(\delta_2^*, \delta_1^*) = 60.9209$ and $d_2(\delta_2^*, \delta^*_{\mathbf{origin}}) = 34.3212$. Using the adaptation algorithm, we can check that $\delta_1^* \in \mathbf{SR}_2$ and $\delta_2^* \in \mathbf{SR_{origin}}$.

3) Simulation results: When there is no control in use, the post-fault dynamics evolve as in Fig. 4 in which we can see that the angle of the load bus 5 significantly deviates from that of other buses with the angular differences larger than 6. This implies that the post-fault dynamics evolve to a different EP instead of the desired stable EP $\delta^*_{\mathbf{origin}}$, where the angular differences are all smaller than 0.6.

We subsequently perform the following control actions:

(i) Changing the power injections of generators 1-3 and controllable load buses 4-6 to $P_1 = 0.5890, P_2 = 0.5930, P_3 = 0.5989, P_4 = -0.0333, P_5 = -0.0617, P_6 = -0.0165$. From Fig. 5 and Fig 6, it can be seen that the bus angles of the post-fault dynamics converge to the EP of the controlled post-fault dynamics which is the first EP δ_1^*. In Fig. 7, we can see that the generator frequencies converge to the nominal frequency, implying that the post-fault dynamics converge to the stable EP δ_1^*. However, it can be seen that the frequencies remarkably fluctuate. The fluctuation happens because we only change the power injection one time and let the post-fault dynamics automatically evolve to the designed EP δ_1^*. This is different from using the AGC where the fluctuation of the generator frequencies is minor, however we need to continuously measure the frequency and continuously update the control.

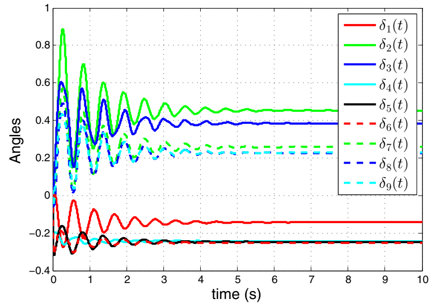

Fig. 8. Effect of susceptance control: Convergence of buses angles from δ_1^* to the second EP δ_2^* in post-fault dynamics.

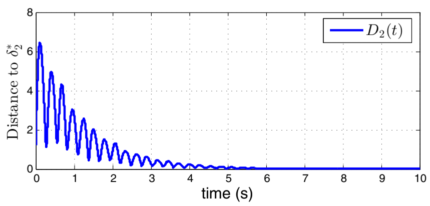

Fig. 9. Effect of susceptance control: the convergence of the distance $D_2(t)$ to 0. Here, the Euclid distance $D_2(t)$ between a post-fault state and the second EP δ_2^* is defined as $D_2(t) = \sqrt{\sum_{i=2}^{9}(\delta_{i1}(t) - \delta_{2_{i1}}^*)^2}$.

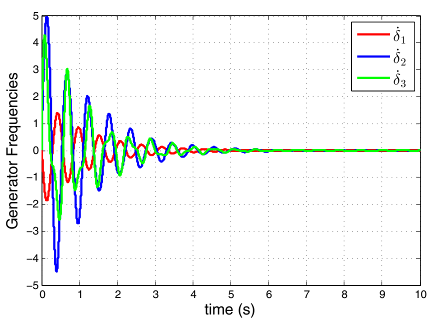

Fig. 10. Generators frequencies under susceptance control.

(ii) To recover the resource spent for the power injection control, we switch the power injections to the original value. At the same time, we change the susceptances of transmission lines $\{1,4\},\{2,7\}$, and $\{3,9\}$ to $B_{14}^{(2)} = 33.4174p.u., B_{27}^{(2)} = 22.1662p.u.$, and $B_{39}^{(2)} = 24.3839p.u.$ The system trajectories will converge from the first EP δ_1^* to the second EP δ_2^*, as shown in Figs. 8-10. In this case we also observe the fluctuation of generator frequencies, which is the result of the one-time change of line susceptances and autonomous post-fault dynamics after this change.

(iii) Switch the susceptances of lines $\{1,4\},\{2,7\}$, and $\{3,9\}$ to the original values. The system trajectories will autonomously converge from the second EP to the original EP as shown in Fig. 11.

VI. Conclusions

In this paper, we presented a novel emergency control for power grids by exploiting the transmission facilities widely available on the grids. In particular, we designed remedial action to recover the transient stability of power systems by adjusting the transmission susceptances of the post-fault dynamics such that a given fault-cleared state, that originally can lead to unstable dynamics, will be attracted to the post-fault EP. Utilizing the Lyapunov function-based stability certificate, we determined suitable amount of transmission lines' susceptance to be adjusted for remedial actions. We showed that the considered control design can be quickly performed through solving a number of convex optimization problems in the form of SDP and convex QCQP. The advantage of this control is that the transmission line's susceptance or power injection only needs to be adjusted one time in each step, and no continuous measurement of system state is required.

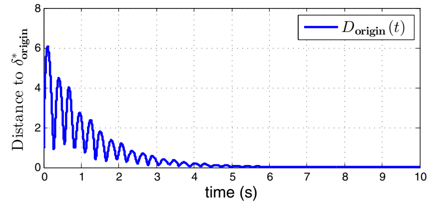

Fig. 11. Autonomous dynamics when we switch the line susceptances to the original values: the convergence of the distance $D_{\mathbf{origin}}(t)$ to 0. Here, the Euclid distance $D_{\mathbf{origin}}(t)$ between a post-fault state and the original EP $\delta^*_{\mathbf{origin}}$ is defined as $D_{\mathbf{origin}}(t) = \sqrt{\sum_{i=2}^{9}(\delta_{i1}(t) - \delta^*_{\mathbf{origin}_{i1}})^2}$.

References

[1] V. Vittal, *Emergency Control and Special Protection Systems In Large Electric Power Systems*. Boston, MA: Birkhäuser Boston, 2003, pp. 293–314.

[2] S. Koch, M. D. Galus, S. Chatzivasileiadis, and G. Andersson, "Emergency control concepts for future power systems," {*IFAC*} *Proceedings Volumes*, vol. 44, no. 1, pp. 6121 – 6129, 2011, 18th {IFAC} World Congress. [Online]. Available: http://www.sciencedirect.com/science/article/pii/S1474667016445854

[3] E. O. Lawrence, K. H. Lacommare, J. H. Eto, K. H. Lacommare, and J. H. Eto, "Cost of power interruptions to electricity consumers in the United States (U.S.)," 2005.

[4] "Final report on the August 14, 2003 blackout in the United States and Canada: Causes and recommendations," *http://energy.gov/sites/prod/files/oeprod/DocumentsandMedia/BlackoutFinal-Web.pdf*.

[5] I. Nagel, L. Fabre, M. Pastre, F. Krummenacher, R. Cherkaoui, and M. Kayal, "High-Speed Power System Transient Stability Simulation Using Highly Dedicated Hardware," *Power Systems, IEEE Transactions on*, vol. 28, no. 4, pp. 4218–4227, 2013.

[6] T. L. Vu and K. Turitsyn, "Lyapunov Functions family approach to transient stability assessment," *IEEE Transactions on Power Systems*, vol. 31, no. 2, pp. 1269–1277, Mar. 2016.

[7] A. R. Bergen and D. J. Hill, "A structure preserving model for power system stability analysis," *Power Apparatus and Systems, IEEE Transactions on*, no. 1, pp. 25–35, 1981.

[8] T. L. Vu, S. M. A. Araifi, M. S. E. Moursi, and K. Turitsyn, "Toward simulation-free estimation of critical clearing time," *IEEE Transactions on Power Systems*, vol. 31, no. 6, pp. 4722–4731, Nov 2016.

[9] T. L. Vu, S. Chatzivasileiadis, H.-D. Chiang, and K. Turitsyn, "Structural emergency control paradigm," *arXiv preprint arXiv:1607.08183*, 2016.

[10] F. Dorfler, M. Chertkov, and F. Bullo, "Synchronization in complex oscillator networks and smart grids," *Proceedings of the National Academy of Sciences*, vol. 110, no. 6, pp. 2005–2010, 2013.

[11] P. M. Anderson and A. A. Fouad, *Power Systems Control and Stability (2nd ed.)*, ser. IEEE Press Power Engineering Series. Piscataway, NJ, USA: John Wiley & Sons, 2003.